Int. J. Heat Mass Transfer. Vol. 15, pp. 2097–2107. Pergamon Press 1972. Printed in Great Britain

FLOW AND HEAT TRANSFER ON A FLAT PLATE NORMAL TO A TWO-DIMENSIONAL LAMINAR JET ISSUING FROM A NOZZLE OF FINITE HEIGHT

H. MIYAZAKI* and E. SILBERMAN†
University of Minnesota, Minneapolis, Minnesota, U.S.A.

(*Received* 2 *August* 1971 *and in revised form* 22 *December* 1971)

Abstract—The two-dimensional laminar jet issuing from a nozzle of half width which terminates at height above a flat plate normal to the jet is analyzed theoretically. The available potential flow solution obtained by conformal mapping is used for the distribution of main-stream velocity over the flat plate. Then, the boundary-layer equations and the energy equation are solved by a finite difference method to evaluate the local friction factor C_f and Nusselt number Nu. Results are presented graphically for the non-dimensional nozzle heights $H = 1{\cdot}0$, $1{\cdot}5$, $2{\cdot}0$, $3{\cdot}0$ and ∞, and for the Prandtl numbers $Pr = 0{\cdot}7$, $1{\cdot}0$, $5{\cdot}0$ and $10{\cdot}0$. The profile of main-stream velocity for $H = 3{\cdot}0$ coincides substantially with that for $H = \infty$; also there are no distinguishable differences between the two cases in the flow-friction and heat-transfer characteristics. C_f varies linearly close to the point of jet impingement as for a stagnation flow in infinite fluid, attains its maximum value, and then approaches asymptotically the value for the flow over a flat plate. C_f increases with decrease in H, and the maximum value for $H = 1{\cdot}0$ reaches approximately $3{\cdot}5$ times the value for $H = \infty$. Nu varies similarly to C_f except close to the point of impingement where it remains constant. The maximum value of Nu for $H = 1{\cdot}0$ is approximately $1{\cdot}7$ times the value for $H = \infty$ so that the increase of flow friction due to small nozzle height is much more remarkable than the enhancement of heat transfer rate.

NOMENCLATURE

C_f, friction factor;
d_i, mesh parameter, $(\xi_{i+1} + \xi_i)/(\xi_{i+1} - \xi_i)$;
$F(\xi, \eta)$, non-dimensional stream function defined by equation (9);
h, nozzle height from the flat plate;
H, non-dimensional nozzle height from the flat plate, h/l;
$I_{i,j}$, quantity defined by equation (26);
k, thermal conductivity;
l, half width of nozzle;
N, number of divisions in the η-direction;
Nu, Nusselt number, $\alpha l/k$;
p_i, velocity defined by $q_{i+1} + q_i$;
Pr, Prandtl number, ν/κ;
q, velocity defined by $\partial F/\partial \eta$;
Re, Reynolds number, $u_\infty l/\nu$;
t, temperature;
T, non-dimensional temperature, $(t_w - t)/(t_w - t_\infty)$;
u, v, velocity components in the x- and y-directions;
U, non-dimensional velocity, u/u_∞;
w_i, temperature defined by $t_{i+1} + t_i$;

* Department of Mechanical Engineering.
† Department of Civil and Mineral Engineering, St. Anthony Falls Hydraulic Laboratory.

x, coordinate along the plate;
X, non-dimensional coordinate along the plate, x/l;
y, coordinate normal to the plate.

Greek symbols

α, heat-transfer coefficient;
$\beta(\xi)$, form parameter defined by equation (13);
γ, constant parameter;
δ, δ_t, boundary-layer and thermal boundary-layer thicknesses;
$\Delta\eta$, mesh size in the η-direction;
η, non-dimensional coordinate defined by equation (8);
κ, thermal diffusivity;
μ, viscosity;
ν, kinematic viscosity;
ξ, non-dimensional coordinate defined by equation (7);
ρ, density;
τ, shearing stress;
ψ, stream function.

Subscripts

0, point of impingement;
∞, nozzle;
f, free surface;
i, j, space subscripts in the ξ- and η-directions;
s, main stream;
w, wall.

1. INTRODUCTION

THE PROBLEM investigated here is the two-dimensional jet emerging from a nozzle into surrounding fluid and impinging on a flat plate normal to the jet. The impinging jets are of great practical interest in many industrial fields. They are applied to the annealing of non-ferrous sheet metals and the tempering of glass. They are also used for the drying of textiles and paper, and, in general, for the local heating or cooling of equipment.

Two general cases of impinging jets can be envisaged, i.e. liquid to gas and liquid to liquid or gas to gas. These are differentiated by the relative importance of gravitational forces and of entrainment. In the first case, liquid to gas, entrainment is negligible and the jet forms a free surface; however, gravity influences the speed. In the second case, entrainment is important and gravity is not so important, especially if the fluids are identical.

After the impingement of the jet on to the flat plate, it spreads out over the surface and a boundary layer develops. Watson [1] classified the flow over the surface into four different regions for a vertical liquid jet with a free surface falling against a plate.

(i) A stagnation region, where the distance x from the point of impingement of the center of the jet is of the order of the half width of nozzle l, and the main-stream velocity u_s rises rapidly from zero to the free-stream velocity u_f. The boundary-layer thickness is of the order of $(\nu l/u_\infty)^{\frac{1}{2}}$ where ν is the kinematic viscosity and u_∞ is the jet speed. For $x \ll l$, the flow in this region can be approximated by the stagnation flow in infinite fluid wherein the main-stream velocity increases linearly with x.

(ii) A flat-plate region at greater distance x where there is practically no pressure gradient in the flow direction and the main-stream velocity is nearly equal to u_f. The flow behavior is essentially identical with that for a flat plate.

(iii) A transition region, where the boundary-layer reaches the free surface, and the entire flow field is subject to viscous stresses. Herein, the velocity profile changes in the flow direction from the flat-plate profile to a fully developed similarity profile.

(iv) A similarity region, where the dimensionless velocity profile remains unchanged, and only the scale varies. In this region the flow becomes independent of the way in which it originated. A hydraulic jump in which the film thickness on the plate increases abruptly will ultimately occur.

The situations are essentially different in the case of a jet discharged into the same fluid, i.e.

liquid into liquid or gas into gas. An entrainment of surrounding fluid by jet is present, and alters the flow of jet before impingement on a flat plate. A stagnation region exists, but far downstream is formed a region called wall jet, where the maximum velocity decreases with x owing to entrainment. There is a transition region between these two regions.

The potential flow solution for an impinging jet on a flat plate was attempted by Michell [2] and Ehrich [3] in conjunction with the flow in valves of various configurations. Their works are summarized in Robertson [4]. It is also discussed in Loitsyanskii [5]. They are, however, interested in the contraction coefficients.

The two-dimensional stagnation flow problem in infinite fluid was first solved by Hiemenz [6], and the solution was improved later by Howarth [7]. The solution for the same problem was obtained by Homann [8], who solved the boundary-layer equations for both the axisymmetric and the two-dimensional laminar flows. Sibulkin [9] followed Homann's similarity transformation and solved the energy equation for the flow near the stagnation point of a body of revolution to evaluate the local Nusselt number. A theoretical analysis for liquid jets with a free surface impinging on a flat plate was made by Watson [1] for both the axisymmetric and the two-dimensional cases with $H = \infty$. Laminar and turbulent flows were considered in all the aforementioned regions except in the stagnation region where a similarity solution ceases to be valid. He also predicted the distance from the stagnation point at which the hydraulic jump occurs, and compared the prediction with experimental results. The problem of heat transfer for impinging liquid jets with $H = \infty$ has been solved by Chaudhury [10], who dealt with axisymmetric laminar flow under various thermal boundary conditions and included frictional heat generation. However, he also avoided the analysis in the stagnation region. Runchal *et al.* [11] applied their numerical technique [12] to solve the Navier–Stokes equations for laminar plane jet impinging on a heated wall for several cases with a fixed nozzle height from the wall under the assumption that streamlines, vorticity and isotherms are parallel to the wall at some downstream location. They presented streamlines, vorticity and temperature patterns, but did not evaluate the friction factor and Nusselt number.

In the present paper, the analysis is confined to the first and second flow regions, i.e. the stagnation and flat plate regions. When a liquid jet discharged into a surrounding of gas impinges on a flat plate, there are no effects of entrainment. However, in the case of liquid jet into liquid or gas jet into gas, the entrainment of surrounding fluid by jet is not negligible. The effects of viscosity in the region of free jet before impingement should be considered in order to estimate the validity of the potential flow solution. They can be ignored if the nozzle height is less than the length of potential core. According to Hrycak *et al.*'s experiment [13] for axisymmetric air jet, the length of potential core is a function of the Reynolds number, and attains the maximum value, 42 nozzle radii, at $Re = 500$, below which the flow is considered to be laminar. It decreases with the decrease of Re, and is 28 nozzle radii at $Re = 300$. In the region of wall jet the maximum velocity decreases along the plate differently from the situation of the potential flow solution, where the main-stream velocity reaches asymptotically the nozzle exit velocity. Consequently, our solution holds up to the transition region between the stagnation and wall-jet regions. In the case of liquid jet into gas our solution is also valid in the flat plate region, i.e. up to the location where the boundary layer thickness reaches the free surface. The location depends on and decreases with Re. Our rough estimation shows that it is 3·3 half nozzle widths at $Re = 100$, and 17 at $Re = 500$. The results of our computation should be, therefore, applicable as an approximation to both liquid jets into gas and jets emerging into a similar ambient fluid.

It is known that the boundary layer in the stagnation region is laminar owing to a positive

pressure gradient even if the jet before impingement is turbulent. Our solution is, however, not valid for the turbulent jet because of the effects of main-stream turbulence which intensifies considerably the flow friction and heat transfer.

The objective of this investigation is to obtain the flow-friction and heat-transfer characteristics on a heated or cooled flat plate against which a two-dimensional laminar jet impinges. The potential flow solution, which is available in [2] and [3], is used for the distribution of main-stream velocity. The solution considers nozzle height from the flat plate. The boundary-layer and energy equations are then solved by a finite difference method after Görtler's transformation, and the local friction factors and Nusselt numbers are evaluated for $H = 1{\cdot}0$, $1{\cdot}5$, $2{\cdot}0$, $3{\cdot}0$ and ∞, and for $Pr = 0{\cdot}7$, $1{\cdot}0$, $5{\cdot}0$ and $10{\cdot}0$.

2. SOLUTION OF THE BOUNDARY-LAYER EQUATIONS

The flow configuration of the impinging jet and the coordinate system are illustrated in Fig. 1.

In order to solve the boundary-layer equations, the distribution of the main-stream velocity u_s is required. To facilitate the understanding of

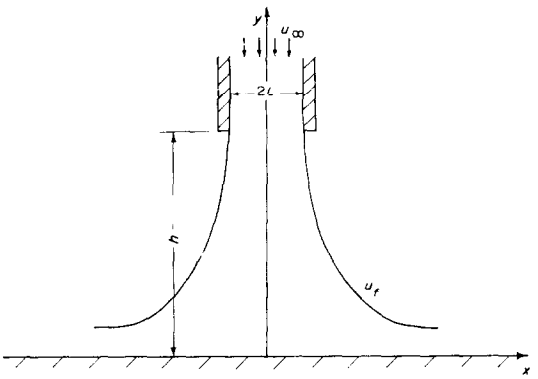

FIG. 1. Flow configuration and coordinate system.

the flow-friction and heat-transfer characteristics, we present here the result derived from the past analysis [3] together with the free-stream velocity u_f. They are given in non-dimensional form as

$$H = \left[1 - \frac{\sqrt{\gamma}}{\pi} \ln \left\{\frac{(\sqrt{\gamma}) - 1}{(\sqrt{\gamma}) + 1}\right\}\right] \Big/ [\sqrt{(\gamma - 1)} + \sqrt{\gamma}], \tag{1}$$

$$U_f = \sqrt{(\gamma - 1)} + \sqrt{\gamma}, \tag{2}$$

$$X = \frac{2}{\pi U_f}\left[\sqrt{(\gamma - 1)} \tan^{-1}\left\{\frac{2\sqrt{(\gamma-1)}U_s/U_f}{1 + (U_s/U_f)^2}\right\} + \ln\left\{\frac{1 + U_s/U_f}{1 - U_s/U_f}\right\} + (\sqrt{\gamma}) \tan^{-1}\left\{\frac{2(\sqrt{\gamma})U_s/U_f}{1-(U_s/U_f)^2}\right\}\right] \tag{3}$$

where γ is a parameter. U_f is only a function of H, and is independent of X. It tends to be infinite in the limit of zero nozzle height. It decreases monotonously with H, and approaches unity asymptotically as H increases.

The distribution of the main-stream velocity

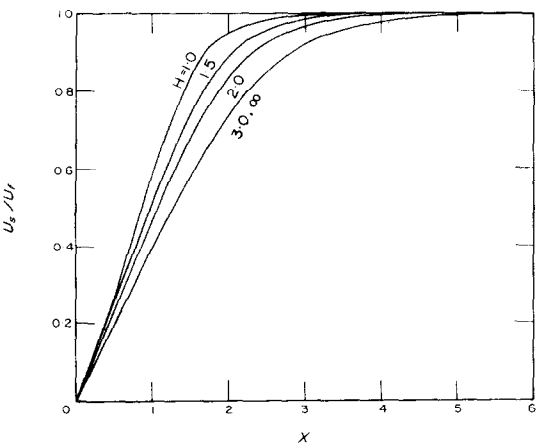

FIG. 2. Distribution of the main-stream velocity for the non-dimensional nozzle heights $H = 1{\cdot}0$, $1{\cdot}5$, $2{\cdot}0$, $3{\cdot}0$ and ∞.

is shown graphically in Fig. 2 for $H = 1{\cdot}0$, $1{\cdot}5$, $2{\cdot}0$, $3{\cdot}0$ and ∞. The curve for $H = 3{\cdot}0$ is seen to agree substantially with that for $H = \infty$. In the close vicinity of the point of impingement, the

flow of the impinging jet may be approximated by the stagnation flow in infinite fluid for which the main-stream velocity increases linearly with X. For infinite nozzle height, the main-stream velocity decreases monotonously, and it approaches the free-stream velocity asymptotically. However, as the nozzle height is reduced the main-stream velocity increases more rapidly than linearly at a distance from the point of impingement which is of the order of the nozzle half-width. This may be explained as follows: when the nozzle is located at infinity so that $U_f = 1$, the flow can spread in the x-direction far ahead of the point of impingement so that the main-stream velocity increases gradually. However, when the nozzle is closer to the plate so that $U_f > 1$ continuity requires a decrease in velocity at the center of nozzle. Further, the decreased clearance between the nozzle and the plate when H is small accelerates the internal flow. Consequently, the main-stream velocity along the plate increases more rapidly closer to the point of impingement than when $H = \infty$.

The boundary-layer equations of continuity and momentum governing the laminar flow with constant properties are given by

$$\frac{\partial u}{\partial x} + \frac{\partial v}{\partial y} = 0, \tag{4}$$

$$u\frac{\partial u}{\partial x} + v\frac{\partial u}{\partial y} = u_s\frac{\mathrm{d}u_s}{\mathrm{d}x} + \nu\frac{\partial^2 u}{\partial y^2} \tag{5}$$

which are subject to the boundary conditions

$$\left.\begin{aligned} u = v = 0 \qquad & \text{at } y = 0, \\ u \to u_s \qquad & \text{as } y \to \infty. \end{aligned}\right\} \tag{6}$$

Here, u and v denote the x- and y-components of velocity respectively. In order to facilitate the numerical analysis, Görtler's transformation is employed

$$\xi = \frac{1}{lu_\infty}\int_0^x u_s(x)\,\mathrm{d}x = \int_0^x U_s(x)\,\mathrm{d}x, \tag{7}$$

$$\eta = \frac{u_s(x)y}{\{2\nu\int_0^x u_s(x)\,\mathrm{d}x\}^{\frac{1}{2}}} = \frac{(\sqrt{Re})U_s(X)\,Y}{\sqrt{2\xi}}, \tag{8}$$

$$F(\xi, \eta) = \frac{\psi(x, y)}{\{2\nu\int_0^x u_s(x)\,\mathrm{d}x\}^{\frac{1}{2}}}, \tag{9}$$

where the Reynolds number is defined by $Re = u_\infty l/\nu$. Using equations (7)–(9), the governing equations (4) and (5) are transformed into the form

$$\frac{\partial^3 F}{\partial\eta^3} + F\frac{\partial F}{\partial\eta} + \beta(\xi)\left\{1 - \left(\frac{\partial F}{\partial\eta}\right)^2\right\} = 2\xi\left\{\frac{\partial F}{\partial\eta}\frac{\partial^2 F}{\partial\xi\partial\eta} - \frac{\partial F}{\partial\xi}\frac{\partial^2 F}{\partial\eta^2}\right\}, \tag{10}$$

with the boundary conditions

$$F = \frac{\partial F}{\partial\eta} = 0 \qquad \text{at } \eta = 0, \tag{11}$$

$$\frac{\partial F}{\partial\eta} \to 1 \qquad \text{as } \eta \to \infty. \tag{12}$$

Here, $\beta(\xi)$ is given by

$$\beta(\xi) = \frac{2\mathrm{d}u_s/\mathrm{d}x\int_0^x u_s\mathrm{d}x}{u_s^2} = \frac{2\xi\mathrm{d}^2\xi/\mathrm{d}x^2}{(\mathrm{d}\xi/\mathrm{d}x)^2}. \tag{13}$$

Taking $q = \partial F/\partial\eta$, equation (10) may be rearranged as

$$\frac{\partial^2 q}{\partial\eta^2} + \left\{\int_0^\eta\left(q + 2\xi\frac{\partial q}{\partial\xi}\right)\mathrm{d}\eta\right\}\frac{\partial q}{\partial\eta} - 2\xi q\frac{\partial q}{\partial\xi} = -\beta(\xi)\,(1 - q^2). \tag{14}$$

In order to solve equation (14), we use the implicit finite difference method developed by Terrill [14]. For details see the reference.

Once the velocity distributions were obtained, the local friction factor is evaluated. It is defined by

$$C_f = \frac{\tau_w}{\frac{1}{2}\rho u_\infty^2}. \tag{15}$$

where ρ is the density, and τ_w is the shearing stress at the wall which is given by

$$\tau_w = \mu\left(\frac{\partial u}{\partial y}\right)_{y=0} = \rho u_\infty^2 \frac{U_s^2}{\sqrt{(2Re\xi)}}\left(\frac{\partial q}{\partial \eta}\right)_{\eta=0}. \quad (16)$$

Inserting equation (16) into (15) and rearranging, we get

$$\tfrac{1}{2}C_f\sqrt{Re} = \frac{U_s^2}{\sqrt{(2\xi)}}\left(\frac{\partial q}{\partial \eta}\right)_{\eta=0}. \quad (17)$$

The first derivative of q with respect to η is replaced by the four-point difference scheme:

$$\left(\frac{\partial q}{\partial \eta}\right)_{\eta=0} = \frac{-11q_{i,0} + 18q_{i,1} - 9q_{i,2} + 2q_{i,3}}{6\Delta\eta}. \quad (18)$$

Consequently, the friction factor is approximated by, with $q_{i,0} = 0$,

$$\tfrac{1}{2}C_f\sqrt{Re} = \frac{U_s^2}{\sqrt{(2\xi)}}\frac{18q_{i,1} - 9q_{i,2} + 2q_{i,3}}{6\Delta\eta}. \quad (19)$$

Figure 3 illustrates the variation of local friction factors as solid lines with the nozzle

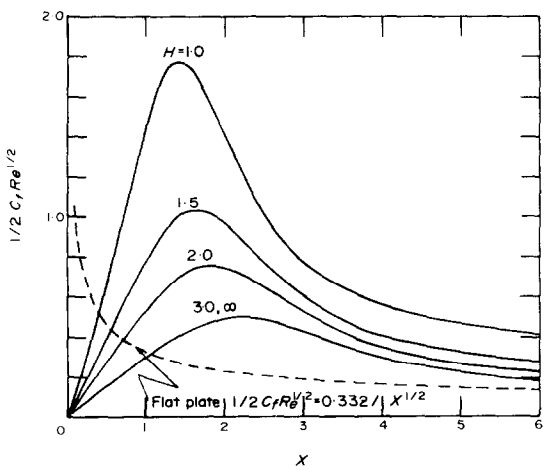

FIG. 3. Variation of the local friction factors for the non-dimensional nozzle heights H = 1·0, 1·5, 2·0, 3·0 and ∞.

height as a parameter, while the dotted line indicates the friction factor for the flow over a flat plate from Schlichting [15]. At the point of impingement, the friction factor is zero, since there is no velocity gradient, and in the immediate vicinity of this point, it increases linearly as in the stagnation flow problem. Far downstream the main-stream velocity approaches a constant value so that the friction factors tend to vary as that for the flow over the flat plate, and to be proportional to the reciprocal of the square root of X. The curves for the impinging jet should coincide with that for the flat plate in the limit by an appropriate choice of fictitious origin. It is interesting to note that, though the main-stream velocity has practically reached a constant value at about $X = 5$, the friction factors there are considerably larger than that for the flow over the flat plate. Maximum values of the friction factor occur for small X because the boundary layer is thin and the main-stream velocity is relatively large there. The maxima are shifted toward the point of impingement with decrease in H since the main-stream velocity approaches the free-stream velocity more rapidly for small H. The maximum values of the friction factors increase significantly with decreasing H owing to the rapid increase in main-stream velocity.

3. SOLUTION OF THE ENERGY EQUATION

The governing equation of energy with the assumptions mentioned in the introduction is

$$u\frac{\partial t}{\partial x} + v\frac{\partial t}{\partial y} = \kappa\frac{\partial^2 t}{\partial y^2} \quad (20)$$

which is subject to the boundary conditions

$$t = t_w \text{ at } y = 0,\ t \to t_\infty \text{ as } y \to \infty. \quad (21)$$

Here, t, t_w, t_∞ and κ are the local, wall, and jet temperatures, and the thermal diffusivity respectively. We now introduce the non-dimensional temperature $T = (t_w - t)/(t_w - t_\infty)$, and then equation (20) is transformed to, using equations (7), (8) and (9):

$$\frac{\partial^2 T}{\partial \eta^2} + PrF\frac{\partial T}{\partial \eta} = 2Pr\xi\left\{\frac{\partial F}{\partial \eta}\frac{\partial T}{\partial \xi} - \frac{\partial F}{\partial \xi}\frac{\partial T}{\partial \eta}\right\}. \quad (22)$$

where Pr is the Prandtl number. The boundary conditions (21) become

$$T = 0 \text{ at } \eta = 0, \qquad T \to 1 \text{ as } \eta \to \infty. \quad (23)$$

Applying the Terrill's finite difference scheme for the boundary-layer equation (14) to the energy equation (22), we have

$$\frac{d^2 w_i}{d\eta^2} + Pr\left[\int_0^\eta \left\{\tfrac{1}{2}p_i + d_i(p_i - 2q_i)\right\} d\eta\right]\frac{dw_i}{d\eta} - Prd_i p_i(w_i - 2T_i) = 0 \quad (24)$$

with $w_i = T_i + T_{i+1}$, where T_i and T_{i+1} are the temperatures at ξ_i and ξ_{i+1} respectively. w_i should satisfy the boundary conditions

$$w_i = 0 \text{ at } \eta = 0,\ w_i \to 2 \text{ as } \eta \to \infty. \quad (25)$$

The derivatives with respect to η are replaced by the central difference scheme, letting

$$I_{i,j} = \int_0^\eta \{\tfrac{1}{2}p_i + d_i(p_i - 2q_i)\}d\eta \approx (\tfrac{1}{2} + d_i)\Delta\eta(p_{i,1} + p_{i,2} + \ldots + \tfrac{1}{2}p_{i,j}) - 2d_i\Delta\eta(q_{i,1} + q_{i,2} + \ldots + \tfrac{1}{2}q_{i,j}). \quad (26)$$

Then, equation (24) is rewritten in the finite difference form as

$$w_{i,j+1} - \frac{2 + \Delta\eta^2 Prd_i p_{i,j}}{1 + (\Delta\eta/2)PrI_{i,j}} w_{i,j} + \frac{1 - (\Delta\eta/2)PrI_{i,j}}{1 + (\Delta\eta/2)PrI_{i,j}} w_{i,j-1} = -\frac{2Prd_i\Delta\eta^2}{1 + (\Delta\eta/2)PrI_{i,j}} p_{i,j}T_{i,j}. \quad (27)$$

Considering the boundary conditions (25), or more specifically $w_{i,0} = 0$ and $w_{i,N+1} = 2$, the first and Nth equations in equation (27) take the forms

$$w_{i,2} - \frac{2 + \Delta\eta^2 Prd_i p_{i,1}}{1 + (\Delta\eta/2)PrI_{i,1}} w_{i,1} = -\frac{2Prd_i\Delta\eta^2}{1 + (\Delta\eta/2)PrI_{i,1}} p_{i,1}T_{i,1}. \quad (28)$$

$$-\frac{2 + \Delta\eta^2 Prd_i p_{i,N}}{1 + (\Delta\eta/2)PrI_{i,N}} w_{i,N} + \frac{1 - (\Delta\eta/2)PrI_{i,N}}{1 + (\Delta\eta/2)PrI_{i,N}} w_{i,N-1} = -\frac{2Prd_i\Delta\eta^2}{1 + (\Delta\eta/2)PrI_{i,N}} p_{i,N}T_{i,N} - 2. \quad (29)$$

The temperature distribution is obtained by solving the system of linear equations which consist of equations (27)–(29). Since the energy equation is linear, there is no need for iterative computations.

The governing equation which gives the temperature distribution at $\xi = 0$ to start the successive computations is

$$\frac{\partial^2 T}{\partial \eta^2} + PrF\frac{\partial T}{\partial \eta} = 0. \quad (30)$$

The solution of equation (30) with the boundary conditions (23) is known in closed form as

$$T = \frac{\int_0^\eta \exp(-Pr\int_0^\eta F d\eta)\ d\eta}{\int_0^\infty \exp(-Pr\int_0^\eta F d\eta)\ d\eta} \quad (31)$$

where F is the solution to the stagnation flow, which was tabulated by Ulrich [16]. The initial temperature distribution was evaluated by the numerical integration of equation (31) for $Pr = 0{\cdot}7$, $1{\cdot}0$, $5{\cdot}0$ and $10{\cdot}0$.

Once the temperature distribution at each increment of ξ was obtained, the Nusselt number may be evaluated. The local heat transfer coefficient α is defined by

$$\alpha(t_w - t_\infty) = -k\left(\frac{\partial t}{\partial y}\right)_{y=0}, \quad (32)$$

where k is the thermal conductivity. Solving equation (32) for α and using the non-dimensional variables, we get

$$\alpha = \frac{k\sqrt{Re}}{l}\frac{U_s}{\sqrt{(2\xi)}}\frac{\partial T}{(\partial\eta)_{\eta=0}}. \quad (33)$$

The local Nusselt number, therefore, becomes

$$Nu = \frac{\alpha l}{k} = \frac{\sqrt{(Re)}U_s}{\sqrt{(2\xi)}}\left(\frac{\partial T}{\partial\eta}\right)_{\eta=0} \quad (34)$$

Approximation of the first derivative with respect to η by the four-point difference scheme, and transfer of the Reynolds number to the left-hand side yield, with $T_{i,0} = 0$,

$$\frac{Nu}{\sqrt{Re}} = \frac{U_s}{\sqrt{(2\xi)}}\frac{18T_{i,1} - 9T_{i,2} + 2T_{i,3}}{6\Delta\eta}. \quad (35)$$

The local Nusselt numbers are shown in Figs. 4–7 as solid lines for $H = 1{\cdot}0$, $1{\cdot}5$, $2{\cdot}0$, $3{\cdot}0$ and ∞ where the dotted lines are those for the flow over the flat plate from Schlichting [15], which are given by

$$\frac{Nu}{\sqrt{Re}} = 0{\cdot}332\,Pr^{\frac{1}{3}}/X^{\frac{1}{2}} \text{ for } 0{\cdot}6 < Pr < < 10. \quad (36)$$

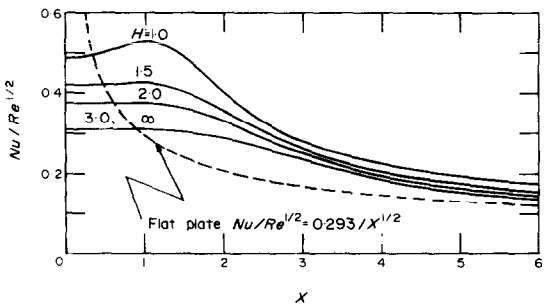

FIG. 4. Variation of the local Nusselt numbers for the non-dimensional nozzle heights $H = 1{\cdot}0$, $1{\cdot}5$, $2{\cdot}0$, $3{\cdot}0$ and ∞ with the Prandtl number $Pr = 0{\cdot}7$.

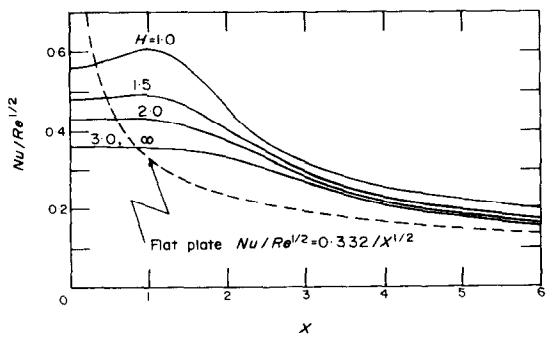

FIG. 5. Variation of the local Nusselt numbers for the non-dimensional nozzle heights $H = 1{\cdot}0$, $1{\cdot}5$, $2{\cdot}0$, $3{\cdot}0$ and ∞ with the Prandtl number $Pr = 1{\cdot}0$.

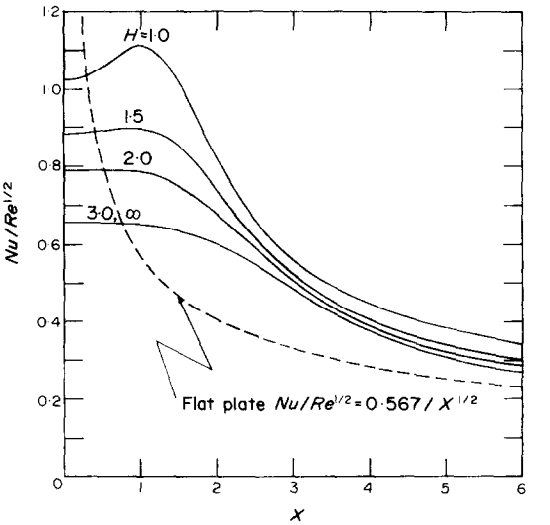

FIG. 6. Variation of the local Nusselt numbers for the non-dimensional nozzle heights $H = 1{\cdot}0$, $1{\cdot}5$, $2{\cdot}0$, $3{\cdot}0$ and ∞ with the Prandtl number $Pr = 5{\cdot}0$.

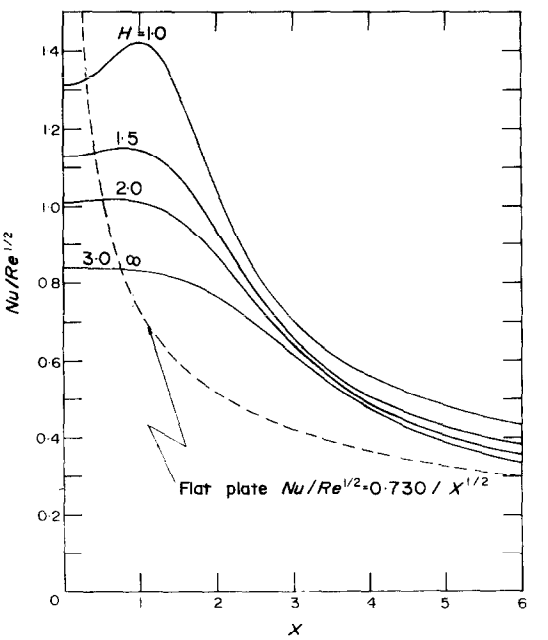

FIG. 7. Variation of the local Nusselt numbers for the non-dimensional nozzle heights $H = 1{\cdot}0$, $1{\cdot}5$, $2{\cdot}0$, $3{\cdot}0$ and ∞ with the Prandtl number $Pr = 10{\cdot}0$.

Figures 4–7 are, respectively, for $Pr = 0{\cdot}7$, $1{\cdot}0$, $5{\cdot}0$ and $10{\cdot}0$.

In the neighborhood of the point of impinge-

ment, the local Nusselt numbers show an essentially different trend than the friction factor. At the origin the friction factor is zero, but the Nusselt number has a non-zero value because there is a temperature difference $t_w - t_\infty$, and heat is transferred by conduction. Moreover, while the former increases linearly the latter remains nearly constant. This is explained by noting that C_f is approximately proportional to u_s/δ where δ is the boundary-layer thickness which is constant, while u_s grows linearly with x; Nu is approximately proportional to $(t_w - t_\infty)/\delta_t$ where δ_t is the thermal boundary-layer thickness which is also constant along with $t_w - t_\infty$.

Far downstream the heat transfer approaches that for the flow over the flat plate, and the Nusselt number decreases in proportion to the reciprocal of the square root of X. At a distance of about the nozzle half-width the Nusselt number is greatly increased for small values of H, and the maximum points of the Nusselt number occur here. Heat transfer is dependent on not only the Reynolds number and the nozzle height but also the Prandtl number, and is enhanced considerably by increase in the Prandtl number because a large Prandtl number means large thermal capacity of the fluid enabling the fluid to carry more heat for the same temperature difference $t_w - t_\infty$. The increase in the Nusselt number due to small H is also more pronounced for large Prandtl numbers.

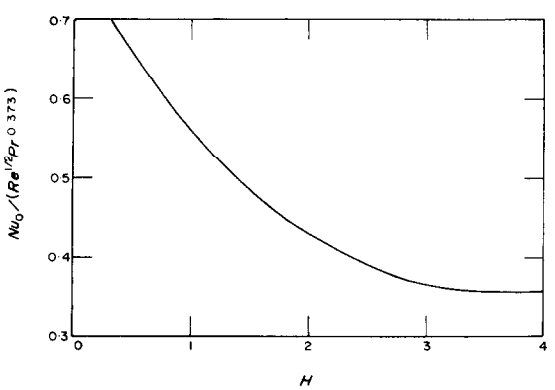

FIG. 8. Correlation of the Nusselt number at the point of jet impingement.

Figure 8 presents a universal correlation curve for the Nusselt number Nu_0 at the point of impingement; this was found to be approximately proportional to $Pr^{0.373}$. The maximum deviation from this curve for all Prandtl numbers is less than 0·9 per cent. According to Sibulkin [9] the Nusselt number at the point of stagnation for a body of revolution is proportional to $P_r^{0.4}$ for $0.6 \leqslant Pr \leqslant 2.0$.

4. CONCLUSIONS

The two-dimensional laminar jet impinging on a flat plate was analysed theoretically. The available potential flow solution obtained by conformal mapping was used for the main-stream velocity over the flat plate for the non-dimensional nozzle heights $H = 1.0$, 1·5, 2·0, 3·0 and ∞. The distribution of main-stream velocity for $H = 3.0$ agrees substantially with that for $H = \infty$. In the immediate vicinity of the point of jet impingement, the main-stream velocity may be approximated by that for stagnation flow in infinite fluid wherein the velocity increases linearly with distance. As H is reduced, the velocity increases more rapidly than linearly when x is near the nozzle half-width.

Using the main-stream velocity, the boundary-layer and energy equations were solved by a finite difference method, and the local friction factors and Nusselt numbers were evaluated. The friction factors increase linearly from zero near the point of impingement, and approach the value for the flow over the flat plate far downstream so that they decrease proportionately to $X^{-\frac{1}{2}}$. In between, maximum values occur and the maximum values of friction factor increase significantly with decrease in H. The Nusselt numbers are greater than zero and remain constant near the point of impingement; for small H, they increase to maximum values shortly beyond impingement.

Far downstream, they tend to vary in proportion to $X^{-\frac{1}{2}}$ as for the flow over the flat plate. The heat transfer depends not only on the Reynolds number and H, as does the friction factor, but also on the Prandtl number; the Nusselt numbers increase considerably with increase in the Prandtl number. The Nusselt number at the point of impingement is found to be approximately proportional to $Pr^{0.373}$.

REFERENCES

1. E. J. WATSON, The radial spread of a liquid jet over a horizontal plane, *J. Fluid Mech.* **20**, 481–499 (1964).
2. J. H. MICHELL, On the theory of free streamline. *Phil. Trans. R. Soc.* **181A**, 389–431 (1890).
3. F. F. EHRICH, Some hydrodynamic aspects of valves, ASME Paper 55-A-114 (1955).
4. J. M. ROBERTSON, *Hydrodynamics in Theory and Application*, pp. 516–523. Prentice-Hall, Englewood Cliffs, New Jersey (1965).
5. L. G. LOITSYANSKII, *Mechanics of Liquid and Gases*, pp. 311–320. Pergamon Press, Oxford (1966).
6. K. HIEMENZ, Die Grenzschicht an einem in den gleichförmigen Flüssigkeitsstrom eingetauchten geraden Kreiszylinder, *Dingl. Polytechn. J.* **326**, 321–324 (1911).
7. L. HOWARTH, On the calculation of the steady flow in the boundary layer near the surface of a cylinder in a stream, ARC RM 1632 (1935).
8. F. HOMANN, Der Einfluss grosser Zähigkeit bei der Strömung um den Zylinder und um die Kugel, *Z. Angew. Math. Mech.* **16**, 153–164 (1936).
9. M. J. SIBULKIN, Heat transfer near the forward stagnation point of a body of revolution, *J. Aero. Sci.* **19**, 570–571 (1965).
10. Z. H. CHAUDHURY, Heat transfer in a radial liquid jet, *J. Fluid Mech.* **20**, 501–511 (1964).
11. A. K. RUNCHAL, D. B. SPALDING and M. WOLFSHTEIN, The numerical solution of the elliptic equations for transport of vorticity, heat and matter in two-dimensional flows, Imperial College, Mech. Eng. Dept. Rep. SF/TN/14 (1968).
12. A. D. GOSMAN, W. M. PUN, A. K. RUNCHAL, D. B. SPALDING and M. WOLFSHTEIN, *Heat and Mass Transfer in Recirculating Flows*. Academic Press, London (1969).
13. P. HRYCAK, D. T. LEE, J. W. GAUNTNER and J. N. B. LIVINGOOD, Experimental flow characteristics of a single turbulent jet impinging on a flat plate, NASA TN D-5690 (1970).
14. R. M. TERRILL, Laminar boundary layer flow near separation with and without suction, *Phil. Trans. R. Soc.* **253A**, 55–100 (1960).
15. H. SCHLICHTING, *Grenzschicht-Theorie*, p. 120 and p. 275. G. Braun, Karlsruhe (1965).
16. A. ULRICH, Die ebene laminare Reibungsschicht an einem Zylinder, *Arch. Math.* **2**, 33–41 (1949).

ECOULEMENT ET TRANSFERT THERMIQUE SUR UNE PLAQUE PLANE NORMALE A UN JET LAMINAIRE BIDIMENSIONNEL SORTANT D'UNE TUYERE DE HAUTEUR FINIE

Résumé—On étudie théoriquement le jet laminaire bidimensionnel sortant d'une tuyère à distance d'une plaque plane normale au jet. La solution de l'écoulement potentiel obtenue par transformation conforme est utilisée pour connaître le champ des vitesses de l'écoulement principal sur la plaque. Les équations de la couche limite et de l'énergie sont ensuite résolues par une méthode aux différences finies pour évaluer le coefficient local de frottement C_f et le nombre de Nusselt Nu. Les résultats sont présentés graphiquement pour les hauteurs adimensionnelles de la tuyère $H = 1{,}0$; 1,5; 2,0; 3,0 et ∞, et pour des nombres de Prandtl $Pr = 0{,}7$; 1,0; 5,0 et 10. Le profil des vitesses du mouvement principal pour $H = 3$ coïncide avec celui pour $H = \infty$; de même il n'y a pas de différence visible entre les deux cas pour les caractéristiques de frottement et de transfert thermique. C_f varie linéairement au voisinage du point d'impact comme pour l'écoulement d'arrêt dans un fluide infini, atteint une valeur maximale puis approche asymptotiquement de la valeur correspondant à l'écoulement sur plaque plane. C_f augmente lorsque H décroît et la valeur maximale pour $H = 1$ atteint approximativement 3,5 fois la valeur pour H infini. Nu varie de façon semblable à C_f sauf près du point d'impact où il reste constant. La valeur maximale de Nu pour $H = 1$ est presque 1.7 fois la valeur pour $H = \infty$ si bien que l'accroissement du frottement dû à une faible hauteur de la tuyère est plus remarquable que celui du flux de transfert thermique.

DIE STRÖMUNG UND DER WÄRMEÜBERGANG AN EINER EBENEN PLATTE SENKRECHT ZU EINEM ZWEIDIMENSIONALEN LAMINAREN STRAHL, DER AUS EINER DÜSE ENDLICHER HÖHE AUSTRITT

Zusammenfassung—Es handelt sich um die theoretische Untersuchung eines zweidimensionalen laminaren Strahles, der aus einer Düse von halber Breite austritt. Die Düse endet über einer ebenen Platte, die senkrecht zum Strahl steht. Die Lösung für die Potentialströmung, die man durch konforme Abbildung erhält, wurde für die Verteilung der Freistromgeschwindigkeit über der Platte herangezogen. Dann wurden die Grenzschichtgleichungen und die Energiegleichung mit einem Differenzenverfahren gelöst, um den Faktor für die lokale Wandreibung C_f und die lokale Nusselt-Zahl Nu zu ermitteln. Ergebnisse

sind graphisch angegeben für dimensionslose Düsenhöhen $H = 1{,}0; 1{,}5; 2{,}0; 3{,}0$ und für Prandtl-Zahlen $Pr = 0{,}7; 1{,}0; 5{,}0$ und $10{,}0$. Das Aussehen der Freistromgeschwindigkeit für $H = 3{,}0$ stimmt im wesentlichen mit dem für $H = \infty$ überein; ebenso gibt es dann keine merklichen Unterschiede zwischen den beiden Fällen in den Charakteristiken für die Wandreibung und den Wärmeübergang. C_f ändert sich linear in der Zone neben dem Punkt, in dem der Strahl auftrifft,—wie bei der Stauströmung im unbegrenzten Strömungsfeld—erreicht sein Maximum und geht dann asymptotisch gegen den Wert für die Strömung über eine ebene Platte. C_f wächst mit abnehmenden H, und der maximale Wert für $H = 1{,}0$ erreicht annähernd das 3,5-fache des Wertes für $H = \infty$. Nu ändert sich ähnlich wie C_f mit Ausnahme der Zone beim Staupunkt, wo der Wert konstant bleibt. Der maximale Wert von Nu für $H = 1{,}0$ ist annähernd das 1,7-fache des Wertes für $H = \infty$, so dass der Anstieg der Wandreibung aufgrund der geringen Düsenhöhe viel stärker ist als die Zunahme des Wärmeübergangs.

ТЕЧЕНИЕ И ТЕПЛООБМЕН ПЛОСКОЙ ПЛАСТИНЫ ПРИ ВЗАИМОДЕЙСТВИИ С ПЕРПЕНДИКУЛЯРНОЙ ДВУМЕРНОЙ ЛАМИНАРНОЙ ПЛОСКОЙ СТРУЕЙ, ИСТЕКАЮЩЕЙ ИЗ СОПЛА НА КОНЕЧНОЙ ВЫСОТЕ

Аннотация—Проводится теоретический анализ двумерной ламинарной струи, перпендикулярной пластине, вытекающей из сопла, расположенного на конечной высоте над пластиной. Для получения распределения скорости основного потока на пластине используется известное решение для потенциального потока, полученное методом конформных отображений. Значения локального коэффициента трения C_f и числа Нуссельта Nu находятся решением уравнений пограничного слоя и уравнения энергии методом конечных разностей. Результаты представлены графически для ряда безразмерных значений высоты сопла: $H = 1{,}0; 1{,}5; 2{,}0; 3{,}0; \infty$, и чисел Прандтля $Pr = 0{,}7; 1{,}0; 5{,}0; 10{,}0$. Профиль скорости основного потока для $H = 3{,}0$ удовлетворительно совпадает с профилем для $H = \infty$. Кроме того не обнаружено заметных различий в характеристиках теплообмена и трения для этих двух случаев. C_f изменяется линейно вблизи точки натекания струи на пластину, как и в случае критического потока в неограниченном объеме жидкости, затем достигает максимальной величины и, наконец, асимптотически приближается к величине C_f при обтекании плоской пластины. C_f возрастает при уменьшении H, достигая своего максимального значения при $H = 1{,}0$, которое примерно в 3,5 раза больше величины C_f при $H = \infty$. Nu изменяется аналогично C_f за исключением области вблизи точки натекания, где оно постоянно. Максимальное значение Nu для $H = 1{,}0$ примерно в 1,7 раза больше его значения при $H = \infty$. Таким образом, при небольших значениях высоты сопла наблюдается более значительное увеличение коэффициента трения по сравнению с ростом теплообмена.